Modeling of a Membrane Reactor System for Crude Palm Oil Transesterification. Part I: Chemical and Phase Equilibrium

Pin Pin Oh
Dept. of Chemical and Environmental Engineering, Faculty of Engineering, University of Nottingham Malaysia Campus, Jalan Broga, Semenyih 43500, Selangor Darul Ehsan, Malaysia

Engineering and Processing Research Div., Malaysian Palm Oil Board, Selangor, Malaysia

Mei Fong Chong
Dept. of Chemical and Environmental Engineering, Faculty of Engineering, University of Nottingham Malaysia Campus, Jalan Broga, Semenyih 43500, Selangor Darul Ehsan, Malaysia

Centre of Sustainable Palm Oil Research (CESPOR), Faculty of Engineering, University of Nottingham Malaysia Campus, Jalan Broga, Semenyih 43500, Selangor Darul Ehsan, Malaysia

Harrison Lik Nang Lau and Yuen May Choo
Engineering and Processing Research Div., Malaysian Palm Oil Board, Selangor, Malaysia

Junghui Chen
Dept. of Chemical Engineering, Chung-Yuan Christian University, Chung-Li, Taiwan 320, Republic of China

DOI 10.1002/aic.14806
Published online April 13, 2015 in Wiley Online Library (wileyonlinelibrary.com)

Using a membrane reactor for reversible transesterification reaction involves reaction and product separation within a single unit. However, a pseudohomogeneous reaction and heterogeneous separation must be maintained for successful membrane reactor operation. Present research is aimed to develop an integrated model of chemical and phase equilibrium (CPE) and modified Maxwell–Stefan equation that describes the simultaneous CPE and mass transport phenomena of biodiesel production from crude palm oil (CPO) using a membrane reactor. In the first part of this work, a systematic approach describing simultaneous CPE of CPO transesterification in the membrane reactor was developed with the reconciliation of transesterification reaction and phase equilibrium that involves six-component. The results revealed that regressed apparent equilibrium constant, K_{eq} value of 17.557±1.51% were higher than the literatures. This indicates that forward reaction of the reversible CPO transesterification is much favored in the membrane reactor than the conventional reactor. © *2015 American Institute of Chemical Engineers* AIChE J*, 61: 1968–1980, 2015*
Keywords: membrane reactor, transesterification, chemical and phase equilibrium, multicomponent, biodiesel

Introduction

Recently, the two-phase membrane reactor technology for simultaneous transesterification reaction and separation to produce high quality biodiesel receives great attention to overcome the problems of poor reaction and purification. Cao et al.,[1] Dubé et al.,[2] and Cao et al.[3] were the earliest group that has reported several research works on biodiesel production via membrane reactor. The membrane reactor technology is able to maintain high mass transfer between the immiscible phases. It combines reaction and separation into a single processing unit to overcome the incomplete conversion as well as downstream purification.[4]

Transesterification is a three-step reversible reaction as

$$\mathrm{TG}+\mathrm{CH_3OH} \underset{k_1'}{\overset{k_i'}{\leftrightarrow}} \mathrm{DG}+\mathrm{R_1COOCH_3} \quad (1)$$

$$\mathrm{DG}+\mathrm{CH_3OH} \underset{k_2'}{\overset{k_3'}{\leftrightarrow}} \mathrm{MG}+\mathrm{R_2COOCH_3} \quad (2)$$

$$\mathrm{MG}+\mathrm{CH_3OH} \underset{k_4'}{\overset{k_5'}{\leftrightarrow}} \mathrm{GLY}+\mathrm{R_3COOCH_3} \quad (3)$$

where TG is triglyceride, DG is diglyceride, MG is monoglyceride, GLY is glycerol, R_iCOOCH_3 is fatty acid methyl ester (FAME), CH_3OH is methanol (MEOH), k_1', k_3', and k_5' are the effective forward rate constants for the catalyzed

Correspondence concerning this article should be addressed to M. F. Chong at meifong.chong@nottingham.edu.my or J. Chen at jason@wavenet.cycu.edu.tw.

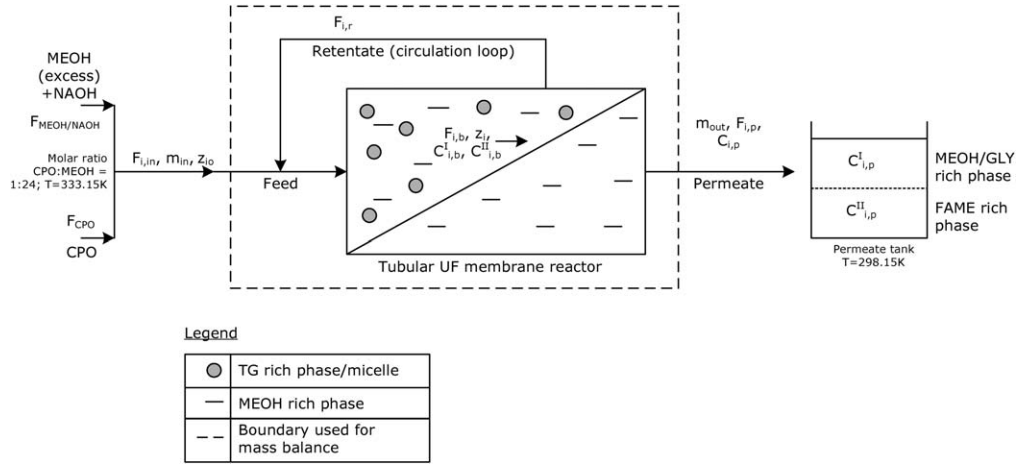

Figure 1. Schematic diagram of CPO transesterification in the membrane reactor prototype.

reactions and $k_2^{'}$, $k_4^{'}$, and $k_6^{'}$ are the effective reverse rate constants for the catalyzed reactions.

In transesterification reaction, oils, MEOH and FAME are partially miscible.[5] During the reaction, reaction mixture passes from a biphasic (MEOH phase and oil phase) system to another biphasic (FAME-rich phase and MEOH/GLY-rich phase) system, probably through an emulsion.[6] This results in a two-phase reaction system causing a mass-transfer limitation for effective reaction. Yet, Dubé et al.[2] proved that the formation of two-phase system is necessary for efficient operation of the membrane reactor.

Zhou and Boocock[6] proposed that MG and DG could more easily access the polar GLY-rich phase while TG preferred to be in the less polar FAME-rich phase. However, Cao et al.[1] claimed that neither TG nor MG was detected in the permeate, which later separated into MEOH/GLY-rich phase and FAME-rich phase. To confirm TG rejection by the membrane reactor, the knowledge of the phase behavior for the multicomponent transesterification system is crucial.[7] Cheng et al.[7] shows that permeate stream to be free of TG with high permeation rate can be achieved when the feed bulk composition of oil-biodiesel-alcohol was controlled within the two-phase zone of the system.

For such a system, it is important to consider the strong interactions between thermodynamics, chemistry, and kinetics, which are the prerequisite for design, investigation and development of the membrane reactor. To achieve successful operation of the membrane reactor, a pseudohomogenous reaction and heterogeneous separation condition must be obtained.

Therefore, chemical and phase equilibrium (CPE) should be computed simultaneously to control the FAME concentration for the two-phase formation by taking into account the changing compositions within the CPE as well as the effects of transesterification reaction. Nevertheless, CPE alone without considering the simultaneous separation of reaction product during the membrane reactor operation is inadequate to describe the simultaneous transesterification reaction and product separation in the membrane reactor. Performance of a membrane reactor system usually deals with specific internal mass balances as well as their equilibrium relationships, transport phenomena and thermodynamic properties that can only be investigated effectively by mathematical models. Therefore, the complete mathematical model describing the membrane reactor for biodiesel production with the integration of CPE and transport phenomena is developed for the first time and becomes the major contribution in this study.

In this two-part article, we present a systematic approach in describing the simultaneous CPE of crude palm oil (CPO) transesterification in membrane reactor in part I, to reconcile the reaction and phase separation conditions as well as to satisfy the strong interactions between thermodynamics, chemistry, and kinetics for biodiesel production using membrane reactor. This article is then extended in Part II to present a mathematical model (modified Maxwell–Stefan model) describing the transport phenomena and separation behavior, which is integrated with CPE model to obtain a complete model for multicomponent two-phase membrane reactor for biodiesel production.

This article focuses on the reconciliation of phase behavior and reaction kinetics within the feed side of the membrane reactor by integrating the liquid–liquid equilibrium (LLE) thermodynamic model and reaction kinetic model through the CPE model. A set of binary interaction parameters required for LLE describing the multicomponent transesterification system was obtained from our previous work through the correlation of experimental phase equilibrium data based on UNIQUAC thermodynamic model.[8] Furthermore, kinetic rate constants were obtained from our previous work, which studies the kinetic modeling for CPO transesterification reaction in the membrane reactor.[9] With these parameters, this article presents a study of CPE of CPO transesterification system in the membrane reactor based on the model developed to reconcile the simultaneous effects of reaction and phase equilibrium, and the CPE model was then evaluated by comparing the model prediction results with the experimental data.

Basis of membrane reactor for transesterification

Consider a schematic representation of the membrane reactor as shown in Figure 1, in which a mixture of MEOH and CPO (represented as TG) with alkali-catalyst sodium hydroxide (NAOH) was continuously fed into the membrane reactor. The molar ratio of CPO:MEOH at the feed side of the reactor is controlled in a way that MEOH becomes the continuous phase (MEOH-rich phase), and the transesterification occurs at the surface of the oil droplets or micelles (oil- or TG-rich phase) formed. The membrane reactor will encounter failure in operation when phase inversion happens, in which the TG becomes continuous phase. The point of phase inversion in a two-phase system can be expressed as[10]

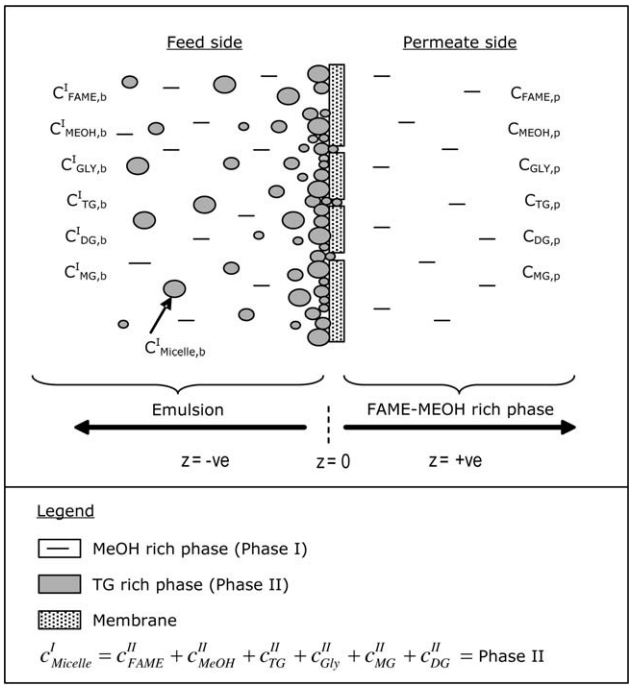

Figure 2. Schematic diagram of forced convection with diffusion to membrane surface in radial or *z*-direction.

$$\frac{\Phi_{\mathrm{MEOH}}}{\Phi_{\mathrm{oil}}} = 1.22\frac{\eta_{\mathrm{MEOH}}}{\eta_{\mathrm{oil}}} \tag{4}$$

The MEOH to TG volume ratio should be maintained at $\frac{\Phi_{\mathrm{MEOH}}}{\Phi_{\mathrm{oil}}} > 0.44$ so that the MEOH is maintained as a continuous phase in the emulsion.[1]

As soon as the transesterification occurs, the FAME/GLY/NAOH that solubilized in MEOH-rich phase with trace amount of TG, DG, and MG will permeate through the membrane following the phenomena as shown in Figure 2. As the oil droplets are too large to pass through the membrane pores, they will be retained on the membrane wall forming a polarization layer, which poses the major mass-transfer limitation for permeation. This is the first assumption made for the transport of a biphasic system through a membrane as illustrated in Figure 2.

Excess of MEOH was used in all experimental runs to ensure that MEOH is the continuous phase. Thus, MEOH is regarded as solvent and other components are regarded as solutes in the process of model development. The components are then taken as the concentrations in the mobile MEOH-rich phase, whereas the TG-rich phase is considered as a single component dispersed as oil droplets or micelle in the MEOH-rich phase. Therefore, the MEOH-rich phase is defined as Phase I and TG-rich phase as Phase II as shown in Figure 2. The concentration of TG, DG, MG, GLY, FAME, MEOH, and micelles in Phase I were denoted as c_i^{I}, in which the superscript I indicates the solutes and solvent concentrations in Phase I. Likewise, the solutes and solvent concentration in Phase II were denoted as c_i^{II} whereby the summation of these concentrations is equated to be the concentration of oil droplet or micelle, which was denoted as $c^{\mathrm{I}}_{\mathrm{Micelle}}$ as shown in Figure 2. Furthermore, we assumed that alkali-catalyst component is negligible during the ultrafiltration in the membrane reactor.

After completion of transesterification reaction, the permeate phase $(c_{i,\mathrm{p}})$ was separated into MEOH/GLY-rich phase and FAME-rich phase once it was cooled down to room temperature at 298.15 K as shown in Figure 1. Subscript p represents the permeate phase. The components concentrations in MEOH/GLY-rich phase are denoted as $c^{\mathrm{I}}_{i,\mathrm{p}}$. Likewise, the components concentrations in FAME-rich phase are denoted as $c^{\mathrm{II}}_{i,\mathrm{p}}$.

By taking the concept as illustrated in Figures 1 and 2, the model of membrane reactor was developed based on several assumptions as follow:

1. The reaction is operated at a function of time until it reaches steady state, and the mixture on retentate side is assumed to be perfectly mixed and recycled back to the feed side of the membrane reactor. The concentration and temperature of the mixture were uniform in the circulation loop of the reactor as shown in Figure 1. This condition can be maintained by controlling the cross flow velocity of 0.75 m/s in the circulation loop.
2. In ideal condition, micelles are fully retained on the retentate side of the membrane due to its larger size than the membrane pores, and it forms a polarization layer.
3. There is no gradient in concentrations, temperature and reaction rate of bulk flow in the radial and axial direction of the tube side of tubular membrane.
4. Excess of MEOH was used to ensure the MEOH becomes the continuous phase. By assuming the alkali-catalyst to be negligible, MEOH is regarded as solvent and other components are regarded as solutes.

Model Development

Chemical and phase equilibrium model development

In the process of CPE model development, component indices based on the order as depicted in Table 1 were used throughout the study. For the transesterification reaction or any other reaction systems, it should satisfy[11]

$$\sum_{i=1}^{n} \beta_{ij} S_i = 0;\ \ j = 1, 2, \ldots, N \tag{5}$$

where i is the component indices based on the order as shown in Table 1. j is the reaction indices with n being the total number of solutes, N is the total number of reaction, which is 6 for reversible transesterification reaction, β is the stoichiometric coefficient where it is defined to have positive values for products and negative values for reactants, and S is the chemical species.

The apparent equilibrium constant, K_{eq} is defined as[12]

$$K_{\mathrm{eq},j} = \prod_{i=1}^{n} \left(\gamma_i^{\mathrm{II}} x_i^{\mathrm{II}}\right)^{\beta_i} = \prod_{i=1}^{n} \left(\gamma_i^{\mathrm{I}} x_i^{\mathrm{I}}\right)^{\beta_i};\ \ j = 1, 2, \ldots, N \tag{6}$$

where x_i^{I} and x_i^{II} are the mole fraction of component i in Phase I and Phase II, respectively. γ_i^{I} and γ_i^{II} are the activity

Table 1. Order of Component *i* in the Bulk Phase of CPE Model

i	Component in Bulk Phase
1	TG
2	DG
3	MG
4	GLY
5	FAME
6	MEOH

coefficient of component i in Phase I and Phase II, respectively, which have taken into account the nonideality in both Phase I and Phase II[13]

By considering Figure 1, the material balance for multiple reactions at steady-state condition is given as[14]

$$F_{i,\text{out}} = F_{i,\text{in}} + \sum_{j=1}^{N} \beta_{ij}\xi_j;\ \ i=1,\ 2,\ \ldots,\ n \tag{7}$$

where F and ξ are defined as the molar flow rate of the species i and the extent of reaction, respectively. The subscripts in is representing inlet to the membrane reactor and out is representing the final flow rate within the membrane reactor, which can be obtained by the summation of retentate $(F_{i,\text{r}})$ and permeate $(F_{i,\text{p}})$ flows.

The reaction of TG-rich phase (dispersed phase) in MEOH-rich phase (continuous phase) formed a liquid–liquid reaction system where a pseudohomogenous system is maintained by efficient mixing so that the residence time of the dispersed phase does not differ much from that of the continuous phase. This is achieved by carrying out the reaction in the membrane reactor in which the dispersion is maintained by turbulence that occurred in the circulation loop and thus the reactions take place at the surface around the dispersed phase. Under this condition, conversion in the dispersed phase is same everywhere due to the same contact/residence time.

Therefore, the objective of this work is to calculate the reaction conversion at the dispersed phase as well as the reactants and products distribution between both phases at equilibrium condition. In this case, the flash equations can be used as the simplified procedure to solve the equilibrium, reactions and material balance of both phases algebraically by taking the phase equilibrium and reaction kinetic relationships as the integral parts of the model. The isothermal flash equations are able to calculate the equilibrium composition between two phases of a mixture at a given temperature and pressure.

A prior specification of possible reactions and their equilibrium constants is required.[12] The Phase I and Phase II are assumed to be in equilibrium, thus the phase equilibrium equations and the flash equations are[12]

$$z_i = \frac{F_{i,\text{b}}}{\sum_{i=1}^{n} F_{i,\text{b}}} = \frac{c_{i,\text{b}} V_\text{o}}{\sum_{i=1}^{n} c_{i,\text{b}} V_\text{o}} \tag{8}$$

$$z_i = \alpha x_i^\text{I} + (1-\alpha) x_i^\text{II} \tag{9}$$

$$x_i^\text{I}\gamma_i^\text{I} = \gamma_i^\text{II} x_i^\text{II} \tag{10}$$

$$x_i^\text{I} = K_i x_i^\text{II} \tag{11}$$

$$\gamma_i^\text{II} = K_i \gamma_i^\text{I} \tag{12}$$

$$\sum_{i=1}^{n} x_i^\text{I} = 1 \tag{13}$$

$$\sum_{i=1}^{n} x_i^\text{II} = 1 \tag{14}$$

where V_o is the reactor volume, $c_{i,\text{b}}$ is the component concentration in the bulk phase of the reactor, K_i is the phase equilibrium ratio for species i and α is the mole fraction of Phase I in the system.

CPE model parameter estimation

Figure 3 presents the algorithm for CPE model parameter estimation. As shown in Figure 3, Eqs. 6–14 can be solved

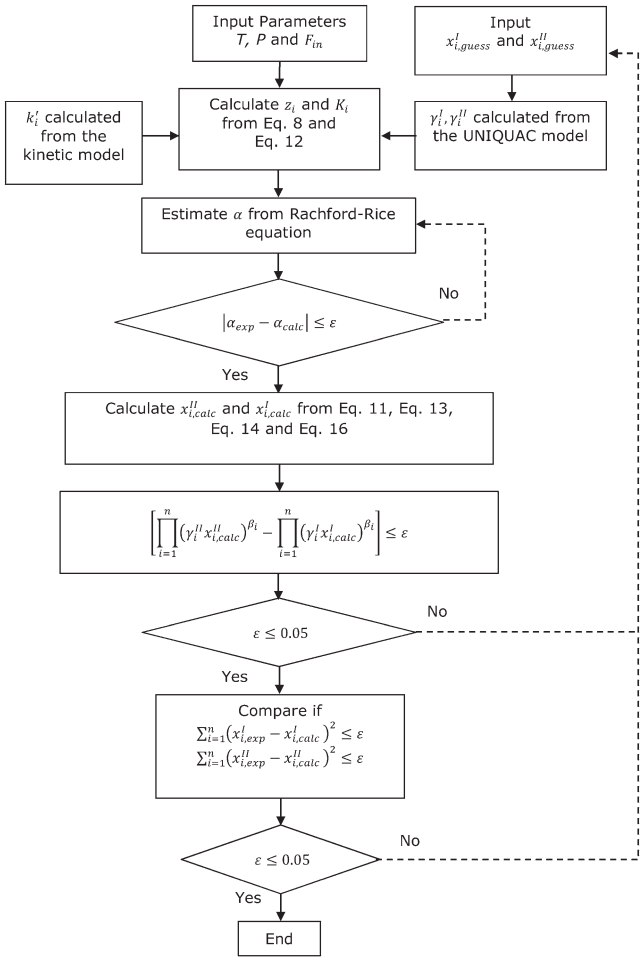

Figure 3. Algorithm for CPE model parameter estimation.

once the values of α, γ, and k_i' are known. The γ value can be correlated from thermodynamic model.[8] The k_i' can be calculated from the reaction kinetic data of CPO transesterification reaction in the membrane reactor.[9] The CPE model was fitted with the experimental data using the genetic algorithm (GA) as the optimization tool of MATLAB.

For a multicomponent liquid mixture, Rachford–Rice equation is often used to calculate the amounts of liquid–liquid in equilibrium with each other at a given temperature and pressure.[15] After the calculation of z_i and K_i from Eqs. 8 and 12, the α value can be estimated from equilibrium isothermal flash calculation that involves solving the Rachford-Rice equation as

$$f(\alpha) = \sum \frac{z_i(1-K_i)}{1+\alpha(K_i-1)} = 0 \tag{15}$$

As the solution of Rachford-Rice equation requires trials-and-error iterative procedure, Newton–Raphson method was used to estimate the α value.

After the equality of α was checked as shown in Figure 3, the equilibrium composition, $x_{i,\text{calc}}^\text{II}$ can be immediately calculated as

$$x_i^\text{II} = \frac{z_i}{1+\alpha(K_i-1)} \tag{16}$$

Subsequently, the $x_{i,\text{calc}}^\text{I}$ can be calculated using Eqs. 11, 13, and 14. The calculated $x_{i,\text{calc}}^\text{I}$ and $x_{i,\text{calc}}^\text{II}$ values are then

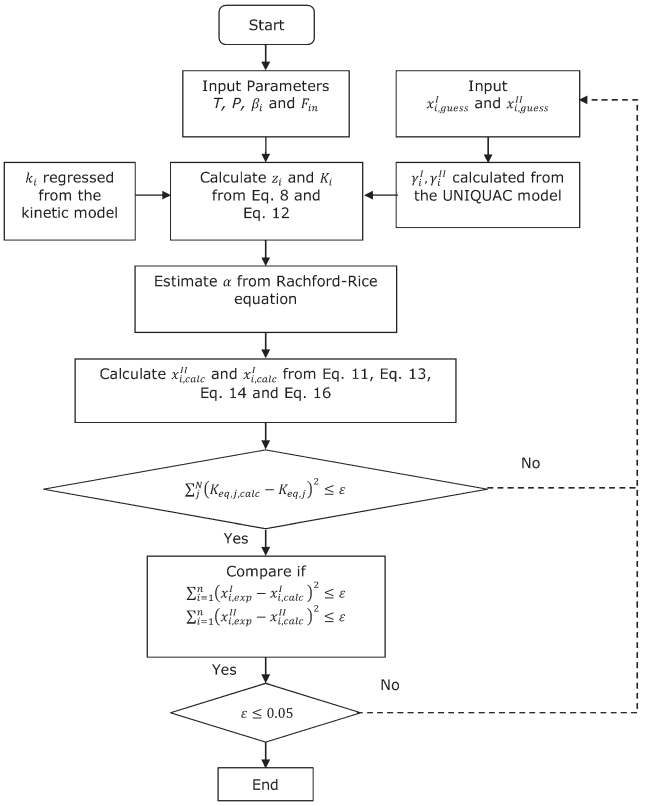

Figure 4. Solution algorithm for CPE model.

substituted into Eq. 6 to estimate the apparent equilibrium constant, $K_{eq,j}$ value for each phase as shown in Figure 3. When the deviation values between the calculated apparent equilibrium constant, $K_{eq,j}$ value for each phase are less than 5%, the goodness of fit was measured by root mean square deviation (RMSD) defined as

$$\text{RMSD} = \left[\sum_{j=I}^{II} \sum_{i=1}^{n} \frac{\left(x^j_{i,\text{exp}} - x^j_{i,\text{calc}} \right)^2}{2n} \right]^{\frac{1}{2}} \quad (17)$$

CPE model solution

Figure 4 presents an overall algorithm to solve the CPE model. Once the Rachford-Rice equation is solved for α, the z_i and K_i can be calculated from Eqs. 11 and 15. The equilibrium composition, $x^{II}_{i,\text{calc}}$ can be immediately calculated from Eq. 16, while x^I_i can be calculated from Eqs. 11, 13, and 14. The calculated x^I_i and x^{II}_i values are then being substituted into Eq. 6 to calculate $K_{eq,j,\text{calc}}$ value and compared with the $K_{eq,j}$ value. The iterative will stop when the deviation values between $K_{eq,j,\text{calc}}$ and $K_{eq,j}$ are less than 5% as shown in Figure 4. If the calculated $K_{eq,j,\text{calc}}$ value is not within the acceptable range, the $x^I_{i,\text{guess}}$ and $x^{II}_{i,\text{guess}}$ values used in the algorithm of are unsuitable and must be updated with new values. When the deviation values between the calculated apparent equilibrium constant, $K_{eq,j,\text{calc}}$ value for each phase are less than 5%, the goodness of fit was measured by RMSD as Eq. 17.

Materials and Methods

Materials

The CPO was obtained from the Malaysian Palm Oil Board (MPOB) Experimental Palm Oil Mill in Labu, Negeri Sembilan, Malaysia. NAOH with a minimum of purity of 98.0% was used in this study. Methanol [high performance liquid chromatography (HPLC) grade, ≥99.9% purity] and acid hydrochloric (HCl), (Grade AR, 37%) were all used as received. The silylating reagent *N,O*-bis(trimethylsilyl) trifluoroacetamide with 1% trimethylchlorosilane (BSTFA) was purchased from Fluka Chemicals (Buchs, Switzerland). All solvents were purchased from Merck (Darmstadt, Germany) and were of HPLC grade.

Methods

Transesterification of CPO with MEOH in the presence of NAOH catalyst was conducted to investigate the CPE of transesterification system and the transport phenomena in the 6 L membrane reactor system as shown in Figure 5. A filtanium™ tubular ceramic membrane (TAMI, Nyons, France) consisting of a titanium oxide support and selective layers was used in the reactor. The tubular membrane with molecular weight cut off (MWCO) of 300 kD used in this study is expected to have the pore size at approximately 0.02 μm as calculated by the size of a 300 kD dextron molecule.[18]. The pore size selected is smaller than the smallest calculated oil droplet size in the membrane reactor for biodiesel production process, which is 12μm as reported by Cao et al.[1]

For all experimental runs, the CPO and MEOH/NAOH were continuously fed to the membrane reactor at a volume ratio of 1:1 basis (CPO:MEOH of 1:24 in molar basis) to have at least an initial 50% volume of MEOH in the reactor. This feed ratio was selected to maintain a continuous MEOH-rich phase within the reactor. Experiments were carried out in varying conditions to study the effects of using different alkali catalyst: 0.05, 0.1, and 0.5 wt % of NAOH by weight of oil (CPO), at constant temperature of 333.15 K and different TMPs. The transesterification conditions used were depicted in Table 2.

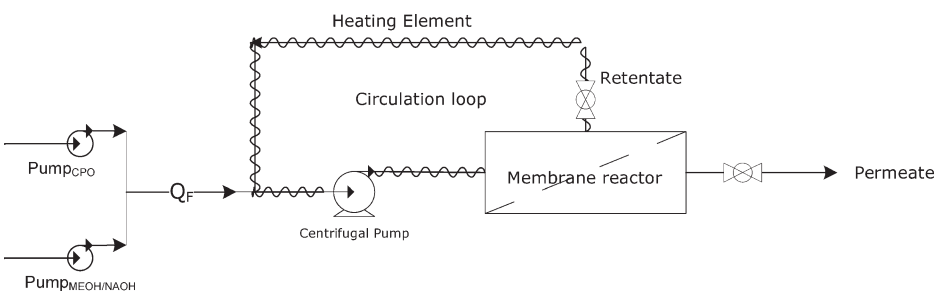

Figure 5. Process flow diagram of membrane reactor prototype system.

Table 2. Experimental Conditions for Transesterification Using Membrane Reactor Prototype at 333.15 K and Reaction Time of 3 h with a Constant CPO:MEOH Molar Ratio of 1:24

Run	Catalyst Concentration (wt %)	TMP (kPa)
1	0.05	103.4
2	0.05	120.6
3	0.05	137.9
4	0.10	103.4
5	0.10	120.6
6	0.10	137.9
7	0.50	103.4
8	0.50	120.6
9	0.50	137.9

First, 6 L of MEOH solution with dissolved NAOH catalyst at predetermined concentration was fed into the membrane reactor system. 3 L of preheated CPO was subsequently fed into the system by displacing the excess 3 L of MEOH/NAOH solution from the reactor. Once the system is filled with both materials, the heating element was turned on to heat up the reactor to 333.15 K. As soon as the centrifugal pump turned on, both the feed pumps were turned on and operated at preset flow rates of 3 L/h, respectively. The pressures of the system were allowed to gradually increase until they reached an initial pressure of 86.2 kPa (12.5 psi), and this took about 15 min. Once the initial pressure was achieved, the valve at the permeate side was opened. Then, permeate began to flow through the membrane, and it was collected at the permeate tank. The TMP of the system were then controlled at predetermined value by regulating the valves at the permeate side and retentate side, monitored, and recorded at predetermined time interval. The feed flow rate and permeate flow rate were also measured at predetermined time interval.

After each experimental run, hot tap water was used to flush the membrane reactor. Once the hot water rinsing was completed, the forward flushing was repeated with pure MEOH solution to ensure all the water was removed from the pipelines and equipment. The membrane permeability was determined with pure MEOH solvent after each forward flushing. Multiple forward flushing was conducted until the initial pure MEOH permeability is recovered to ensure the tubular membranes are properly cleaned.

During the reaction, two sets of samples were collected each at retentate and permeate side of the membrane reactor at predetermined time intervals. For all the experimental runs, the total reaction time was 3 h. As the reaction proceeds in a rapid manner in the first 60 min, samples were collected at every 10 min intervals. Subsequently, samples were collected at every 30 min interval. The samples were quenched immediately using MEOH containing HCL solution. Samples collected at retentate side were considered as bulk phase, and they were allowed to settle into two phases for 1 h, that is, Phase I (MEOH-rich phase) and Phase II (TG-rich phase) at temperature of 333.15 K. Whereas, the samples collected at permeate side were allowed to separate into a MEOH-rich phase and a FAME-rich phase at temperature of 298.15 K.

For the first set of sample, volumes of both phases were measured, and MEOH content in both phases of the sample was determined. For the second set of sample, about 1.0 mL of sample was withdrawn from each phase and dried with compressed nitrogen gas to remove MEOH. The concentrations of TG, DG, MG, GLY, and FAME were measured with the GC-flame ionization detector (FID) method. Thus, component composition for each phase collected at different predetermined time intervals can be obtained. Experimental runs used for parameter regression and validation for different models was tabulated in Table 3. The errors involved in the experiments were calculated in term of overall mass balance analysis based on the measured concentrations and were maintained at ±5%. All experimental runs were conducted in duplicate to obtain average data with the standard deviation maintained at ±5%.

Table 3. Experimental Runs Used for Model Parameter Regression and Validation

Model	Part of Paper	Parameter regression	Model validation
CPE model	I	Run 1, 4, 7	Run 2, 3, 5, 6, 8, 9
Maxwell–Stefan model	II	Run 1, 4, 7	Run 2, 3, 5, 6, 8, 9

Analysis

The GC-FID test method is in accordance with the ASTM D6584 test method for determination of glycerine, glycerides and ester in B-100 biodiesel methyl esters. This method has been tested for about 12 years in the Palm Diesel Quality Control Laboratory of the MPOB for numerous analyses of oil samples.[19]

A 0.02 g of sample was weighed accurately into a 2 mL GC vial. Then, 1.2 mL of dichloromethane and 0.3 mL of the silylating reagent, *N,O*-bis(trimethylsilyl) trifluoroacetamide (BSTFA) with 1% trimethylchlorosilane was pipetted into the vial contains experimental glyceride samples to give derivatives of enhanced volatility and make the derivatives suitable for analysis by gas chromatography (GC). Perkin Elmer AutoSystem XL GC with a flame ionization detector (GC-FID) was used for simultaneous determination of components including TG, DG, MG, FAME, and GLY.[20,21] The GC uses an SGE forte BPX 5 fused-silica capillary column (15 m × 0.32 mm), which was coated with 5% of phenyl or 95% of polysilphenyl-siloxane, with a film thickness of 0.25 μm. Quantification of the components was performed using a five-point external standard calibration assay, with R^2 values of >0.99.

Results and Discussion

CPE model parameter estimation

The CPE model developed in this study was fitted to the experimental data obtained from the CPO transesterification reaction in the membrane reactor. The CPE model parameter regression requires the fitting of apparent equilibrium constant, K_{eq}, which is the only fitting parameter as the reaction rate constants, $k_i^{'}$ and adjustable parameters, A_{ij} were estimated from the kinetic[9] and LLE[15] modeling studies, respectively.

The K_{eq} was determined based on the equilibrium component compositions in each phase, which were calculated from the kinetic data of overall component compositions at equilibrium state. Therefore, similar experimental runs used in the kinetic model parameter regression study were used for the CPE model parameter regression, which were the experimental runs of 1, 4, and 7 as shown in Table 3. Owing to DG and MG are the minor components with very low concentrations as shown in the kinetic modeling study, it is

Table 4. K_{eq} Values Obtained from Existing and Literature Studies for Various Transesterification Reactions

T (K)	Material/ reactor	Catalyst	Catalyst conc. (wt %)	K_{eq}	RMSD (%)	Refs.
333.15	Crude palm oil, methanol/ Membrane reactor	NAOH	0.05	17.504	1.51	Present work
			0.1	17.352	1.87	
			0.5	17.815	1.35	
			Average	17.557(±5%)	N/A	
333.00	Palm oil, isoprophyl ether solution of methanol/ Fixed-bed integral reactor	CaO/ $CaCO_3$	N/A	0.220	N/A	16
333.15	Soybean oil, methanol/ Packed bed reactor	KF/ Ca—Mg—Al hydrotalcite	N/A	3.500	N/A	17
333.15	Canola oil, methanol/ Continuous stirred tank reactor	NAOH	N/A	3.210	N/A	8

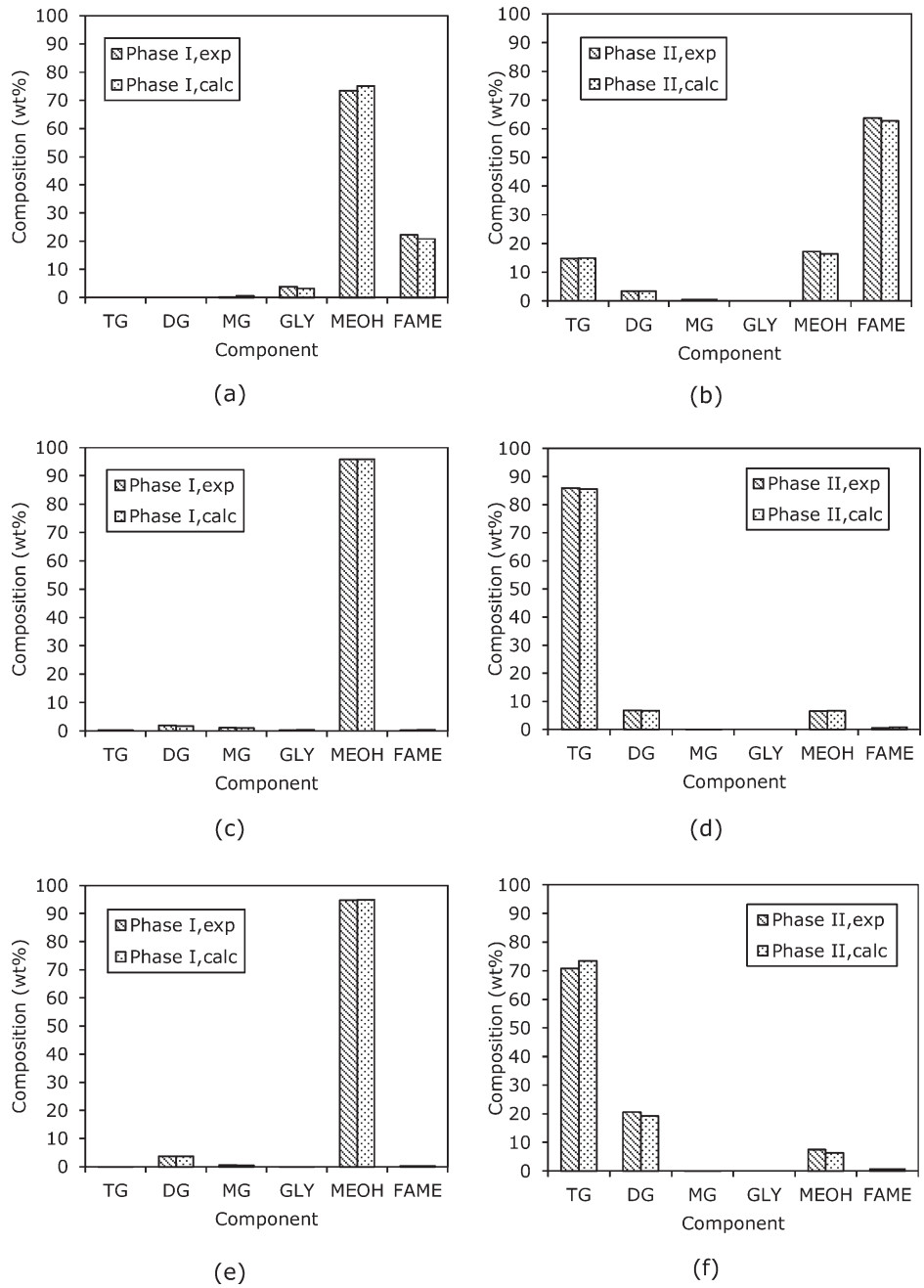

Figure 6. Experimental and CPE model simulation results of components compositions obtained for reactions that used different catalyst concentration of (a,b) 0.5 wt %, (c,d) 0.1 wt %, and (e,f) 0.05 wt % at CPO:MEOH molar ratio of 1:24, temperature of 333.15 K and TMP of 103.4 kPa.

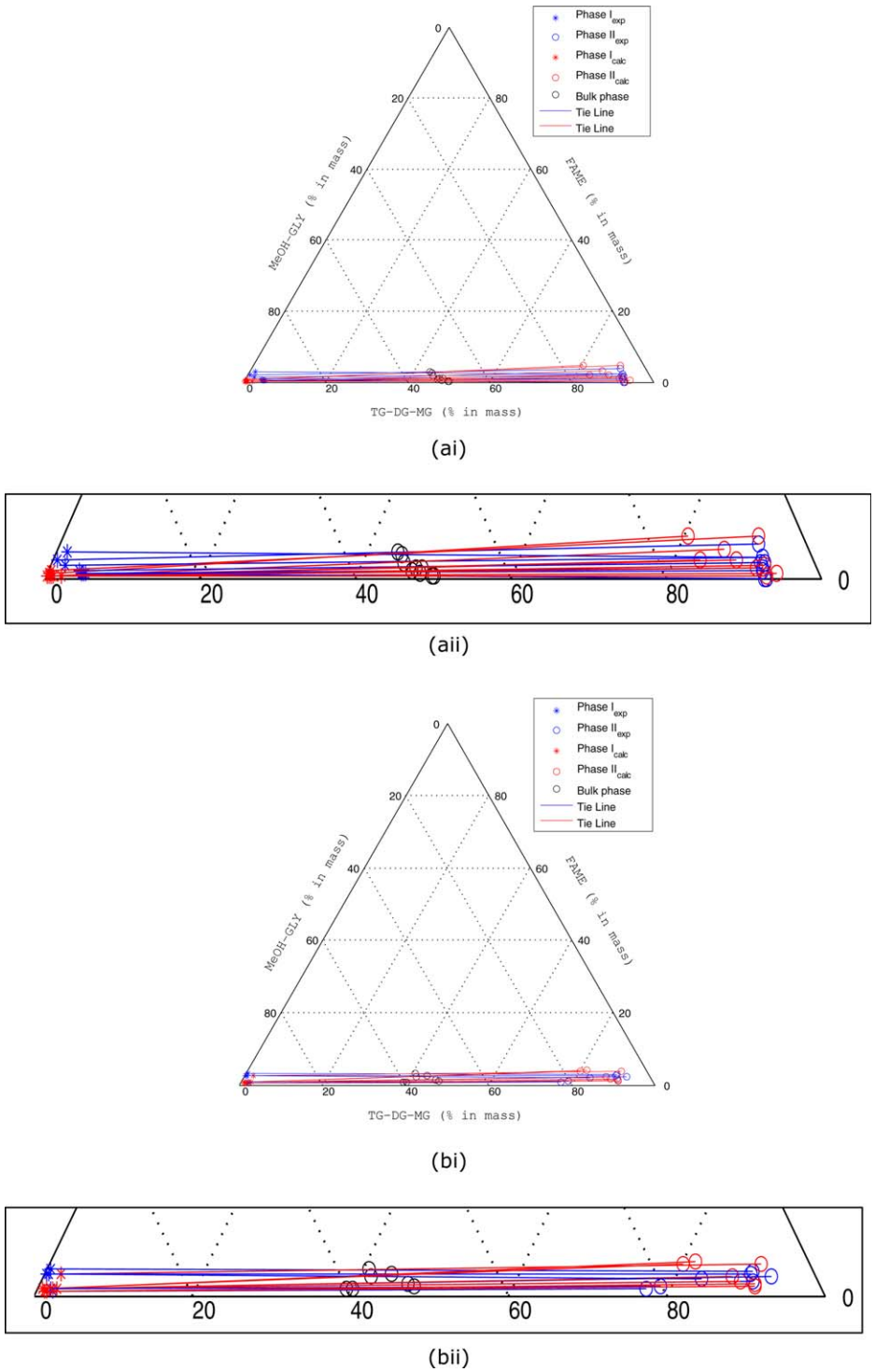

Figure 7. Pseudo-ternary phase diagram for experimental data (exp) and CPE predicted results (calc) for the six-component TG-DG-MG + MEOH-GLY + FAME system at constant CPO:MEOH molar ratio of 1:24, temperature of 333.15 K and TMP of 120.6 kPa with different catalyst concentration of (a) 0.05 wt %, (b) 0.1 wt % and (c) 0.5 wt %. Diagram (aii) and (bii) show the enlarged lower section of respective diagram (ai) and (bi).

[Color figure can be viewed in the online issue, which is available at wileyonlinelibrary.com.]

reasonable to calculate the apparent equilibrium constant based on the overall reaction, whereby the elementary reaction steps were combined. The K_{eq} results obtained from the CPE model fitting using experimental data were tabulated in Table 4 with RMSD values ranging from 1.3–1.9%.

Figure 6 shows the component compositions of TG/DG/MG/GLY/MEOH/FAME in Phase I and Phase II at the feed side of membrane reactor that reacted at CPO:MEOH molar ratio of 1:24 with different catalyst concentration of 0.05, 0.1, and 0.5 wt % at constant temperature of 333.15 K and

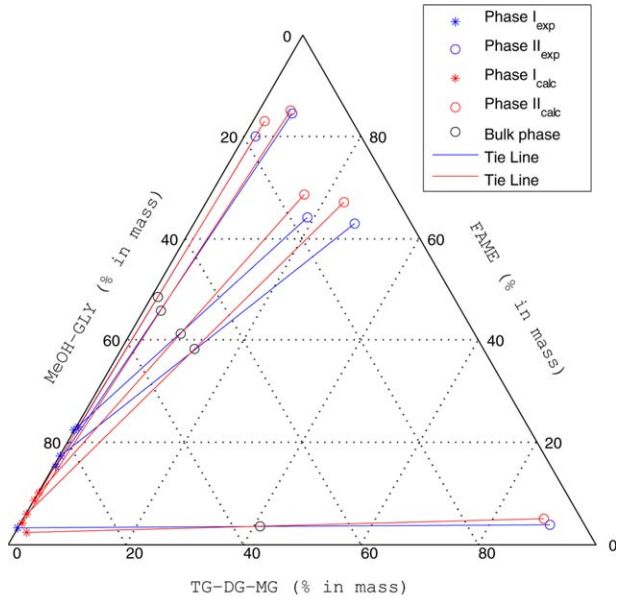

(c)

Figure 7. (Continued)

constant TMP of 103.4 kPa. The good fit between the simulated results and the experimental data as illustrated in the Figure 6 shows that the CPE model parameter regression results as tabulated in Table 4 were satisfying. The conversions obtained are very low for a ratio of CPO:MEOH of 1:24, at the catalyst concentrations used 0.1 and 0.05 wt%. The CPO used in this study consists of 0.15–0.5 % max of moisture content and impurities as well as FFA content of 3.3–4.5 wt % of oil basis. In this case, the catalyst was consumed by the FFA in the present of moisture to form soap. Thus, the catalyst concentration became too low for efficient reaction.

It is reported in Table 4 that the K_{eq} values were almost constant as the catalyst concentration used in the CPO transesterification reaction increased. This finding can be supported by similar results reported in several literatures,[13,22,23] which have investigated the effect of catalyst loading on the apparent equilibrium constant calculation. The results of K_{eq} obtained in this study explain that the use of catalyst only accelerates and helps to attain equilibrium rapidly for the reversible CPO transesterification in the membrane reactor but do not affects the equilibrium shift in the system. Thus, the K_{eq} values obtained in the present work further confirm the Le Chatelier's principle in which the reaction equilibrium is a function of temperature only but not of catalyst concentrations and this is also supported by the finding reported by Forsythe and Parsons.[24]

Since the K_{eq} values obtained from different catalyst concentration were consistent and fall within the $\pm 2\%$ error boundary, an average value of K_{eq} of $17.557 \pm 2\%$ was used in the all the subsequent works of this study. The comparison between the K_{eq} values obtained from existing work and literatures were tabulated in the Table 4. It is clearly seen that the average value of K_{eq} obtained from the present work is different from the literature values and there is no uniqueness for the apparent equilibrium constant values observed from all the studies.

At equilibrium, the standard Gibbs free energy change equation, $\Delta G^{\circ} = -RT\ln K_{eq}$ relates the equilibrium composition of a chemical reaction system to measurable physical properties of the reactants and products.[25,26] Though transesterification reactions were conducted at identical reaction temperature, different types of feedstocks and substances used in the transesterification reactions have different entropies and enthalpy of formations. This generates different standard Gibbs free energy change of the reaction and thus different apparent equilibrium constant values were obtained. This statement clearly explains the different K_{eq} values obtained from reactions that used different feedstocks and substances that exhibit different physical and chemical properties as shown in Table 4.

Furthermore, it is important to note that the K_{eq} value obtained from present work is clearly higher as compared to the literature values as tabulated in Table 4. High apparent equilibrium constant shows that the forward reaction of reversible CPO transesterification reaction in the membrane reactor is favored. This shows that the regressed K_{eq} value from the CPE model is in agreement with the rate constants obtained from the developed kinetic model. This finding also confirms that the role of membrane reactor in reaction products separation to shift the reaction toward the favorable path.

CPE model validation

The regressed apparent equilibrium constant, $K_{eq}$was further validated in the prediction of CPE model using another independent sets of experimental data (run 2, 5, and 8 as shown in Table 3), which were also the similar experimental runs used for the kinetic model validation. The time-dependent experimental data obtained during the CPO transesterification reaction and CPE predicted results were transposed into pseudoternary phase diagrams as shown in Figure 7. Raw data of Figure 7 were tabulated in Appendix A.

A good agreement between the experimental data and predicted results was observed in all the experimental runs with

Table 5. Experimental and Simulation Results of Mole Fraction of Phase I in the Feed Bulk System at Constant Temperature of 333.15 K and Steady State

Catalyst conc. (wt %)	TMP (kPa)	α_{exp}	α_{calc}	Deviation (%)
0.05	103.4	0.9000	0.9009	0.10
	120.6	0.9080	0.9226	1.61
	137.9	0.9075	0.9025	0.55
0.1	103.4	0.9093	0.9080	0.14
	120.6	0.8477	0.8581	1.23
	137.9	0.9105	0.9128	0.25
0.5	103.4	0.8231	0.8219	0.15
	120.6	0.8095	0.8101	0.07
	137.9	0.7982	0.8074	1.15

the RMSD values ranges from 1.3–1.5% that is less than 5%. The good match between CPE model predicted results and experimental data shows that the CPE model with regressed apparent equilibrium constant, K_{eq} can be used to describe and predict the CPE accurately for the six-component CPO transesterification reaction in the membrane reactor.

It can be observed in Figure 7a, b that tie lines representing the LLE of each reaction time were overlapping with each other, which indicates that no variation between the two phases of reaction mixtures at constant CPO:MEOH molar ratio of 1:24 with catalyst concentration of 0.05 and 0.1 wt %, respectively. Furthermore, Figure 7a and b also show that most of the FAME solubilized in TG-rich phase (Phase II) when the reaction mixture had a high TG composition. This situation is undesirable because a mixture with high TG composition will not make efficient separation of FAME from TG in the membrane reactor.

This is because the membrane reactor will reject FAME that solubilizes in Phase II during the separation process. Cao et al.[1] and Cao et al.[3] conducted researches on the phase behavior of transesterification reaction system. They reported that the oil rich phase and alcohol rich phase would form an emulsion during the reaction in which oil rich phase or TG rich droplets (referred as Phase II or micelles in this study) will be dispersed in the continuous phase, i.e. alcohol rich phase (referred as Phase I in this study). The FAME formed will then diffused from the surface of TG rich droplets into Phase I. To have efficient product separation, the FAME concentration in Phase I should be maintained at its highest achievable concentration.

As shown in Figure 7c, it is interesting to note that at this reaction condition, the tie lines shift gradually from the "TG-DG-MG" axis toward the "MEOH-GLY" axis as the reaction time increased. This indicates that as the reaction progressed, the FAME formed was more solubilized in the TG-rich phase at the beginning of the reaction, had finally become the FAME-rich phase when the TG was gradually being reacted with the MEOH along the reaction. It is noticeable in Figure 7c that FAME formed its own phase with very low TG concentration of less than 1.0 wt % for the reaction mixture with CPO:MEOH molar ratio of 1:24 and catalyst concentration of 0.5 wt %. However, the FAME concentration in Phase II, which contains of TG, DG, and MG concentrations, was always higher than Phase I. Nonetheless, TG component was undetectable in Phase I in all the experimental runs depending on the CPE condition as shown in Figure 7 as well as Figure 6. This observation is desirable if an efficient reaction and simultaneous product separation need to be achieved in the membrane reactor.

Controlling the CPE at the feed side of membrane reactor

The concept behind in obtaining the high membrane separation efficiency is depending on the formation of micelles, in which the TG free permeate can only be obtained when the CPE is controlled in such a way that the continuous phase must be free from TG and the micelles or dispersed phase should be large enough to be rejected by the membrane.

Table 5 depicted the simulation results of mole fraction of Phase I, α in the feed bulk system at steady state, which obtained from the CPE modeling study at operating condition of varying catalyst concentration and TMP. The values of α are used to determine the amount of FAME solubilized in Phase I once the compositions of both phases are known. It is noticed from Table 5 that a good agreement between the experimental and predicted results of α values with the deviation values of less than 5%. The results show that 80–92 mol % of Phase I present in the feed side of the membrane reactor whereby the feed bulk concentrations were within the heterogeneous phase zone. Although the FAME content in the Phase I is lower than that in Phase II, more FAME can be solubilized in Phase I as shown in Table 5 due to the higher α values obtained in all runs. Besides, the results tabulated in Table 5 show that constant α were obtained for all the simulation runs at varying catalyst concentration and TMP. This shows that the effects of catalyst concentration and TMP on the α were negligible when high CPO:MEOH molar ratio was used.

The CPE modeling and simulation results obtained in this study show that the CPE modeling is important to provide the information needed for controlling the reaction and phase separation simultaneously. The major outcome of the CPE analysis in this study shows that if the feed bulk concentration of the membrane reactor needs to be controlled within the heterogeneous phase zone as shown in Figure 7c for efficient reaction and product separation, the reaction conditions need to be maintained at constant CPO:MEOH molar ratio of 1:24, catalyst concentration of 0.5 wt % and temperature of 333.15 K. Under these conditions, more FAME will diffuse into the TG-free Phase I and permeate through the membrane as the continuous phase. At the same time, Phase II, which is rich with TG-DG-MG will be retained by the membrane as micelles.

Conclusions

A general approach has been developed in this work for simultaneous CPE modeling. With the parameters of activity coefficients and effective rate constants regressed from UNIQUAC thermodynamic model and kinetic model developed in the previous works, a systematic CPE model was successfully developed for the first time to simulate the simultaneous CPE of CPO transesterification in the membrane reactor, which gives a good fit to the experimental data for all the conditions tested.

The values of K_{eq} were greater than the literatures as the forward reactions of the reversible CPO transesterification are much favored in the membrane reactor than the conventional reactor. With the regressed chemical apparent equilibrium constant, K_{eq} obtained from the CPE model, the model is able to predict the equilibrium compositions and phase behavior at the feed side of the membrane reactor system with high prediction capability. In the second part of this two paper series, we study the mass transport phenomena modeling of CPO transesterification reaction in the membrane reactor.

Acknowledgment

The authors thank the management of Malaysian Palm Oil Board (MPOB) for providing financial support for this study. Technical assistance by the staffs of Biodiesel Technology Group of MPOB is deeply appreciated.

Abbreviation

ASTM = American Society for Testing and Materials
BSTFA = *N,O*-bis(trimethylsilyl) trifluoroacetamide with 1% trimethylchlorosilane
CPE = Chemical and Phase Equilibrium
CPO = Crude Palm Oil
DG = Diglyceride
FAME = Fatty Acid Methyl Ester
FFA = Free Fatty Acid
FID = Flame Ionization Detector
GA = Genetic Algorithm
GC = Gas Chromatography
GLY = Glycerol/Glycerine
HCl = Hydrochloric Acid
LLE = Liquid-Liquid Equilibrium
MEOH = Methanol
MG = Monoglyceride
MPOB = Malaysian Palm Oil Board
MWCO = Molecular Weight Cut Off
NAOH = Sodium Hydroxide
TG = Triglyceride
TMP = Transmembrane Pressure
UNIQUAC = UNIversal QUAsiChemical

Notation

A = Adjustable parameter in UNIQUAC model, -
c = Molar concentration, mol L^{-1}
F = Molar flow rate, mol min^{-1}
k' = Effective rate constant, L mol^{-1} min^{-1}
K = Phase equilibrium ratio, -
K_{eq} = apparent equilibrium constants, -
M_{NAOH} = Molarity of standard NAOH solution, mol mL^{-1}
n = Number of components, -
t = time, min
V_o = Volume of reactor, L
x = mole fraction, -
X = Phase II, -
Y = Phase I, -
z = mole fraction in bulk phase / total system, -

Greet letters

γ = Activity coefficient, -
ε = Error, -
α = Mole fraction of Phase I in the system, -
ξ = Extent of reaction, mol min^{-1}
β = Stoichiometric coefficient, -

Subscripts

b = Bulk phase
calc = Calculated value
CPO = Crude palm oil
exp = Experimental value
F = Feed
guess = Guess value
in = Inlet to the reactor
i, j, k = individual component/solute
j = reaction indices
max = Maximum
MEOH = Methanol
MEOH/NAOH = Solvent of methanol and NAOH

Superscripts

I = Phase I
II = Phase II
k = Number of iteration

Literature Cited

1. Cao P, Tremblay AY, Dubé MA, Morse K. Effect of membrane pore size on the performance of a membrane reactor for biodiesel production. *Ind Eng Chem Res*. 2007;46(1):52–58.
2. Dubé MA, Tremblay AY, Liu J. Biodiesel production using a membrane reactor. *Bioresour Technol*. 2007;98(3):639–647.
3. Cao P, Dubé MA, Tremblay AY. Methanol recycling in the production of biodiesel in a membrane reactor. *Fuel*. 2008;87(6): 825–833.
4. Cao P, Dubé MA, Tremblay AY. High-purity fatty acid methyl ester production from canola, soybean, palm, and yellow grease lipids by means of a membrane reactor. *Biomass Bioenergy*. 2008;32(11):1028–1036.
5. Stavarache C, Vinatoru M, Nishimura R, Maeda Y. Fatty acids methyl esters from vegetable oil by means of ultrasonic energy. *Ultrason Sonochem*. 2005;12(5):367–372.
6. Zhou W, Boocock DGB. Phase behavior of the base-catalyzed transesterification of soybean oil. *J Am Oil Chem Soc*. 2006;83(12): 1041–1045.
7. Cheng L-H, Cheng Y-F, Yen S-Y, Chen J. Ultrafiltration of triglyceride from biodiesel using the phase diagram of oil–FAME–MeOH. *J Membr Sci*. 2009;330(1–2):156–165.
8. Chong MF, Chen J, Oh PP, Chen Z-S. Modeling study of chemical phase equilibrium of canola oil transesterification in a CSTR. *Chem Eng Sci*. 2013;87(0):371–380.
9. Oh PP. *Modelling of a Membrane Reactor System for Crude Palm Oil Transesterification*, Ph.D. Dissertation. University of Nottingham, Malaysia Campus; 2014.
10. Ho RM, Wu CH, Su AC. Morphology of plastic/rubber blends. *Polym Eng Sci*. 1990;30(9):511–518.
11. Fogler HS. *Elements of Chemical Reaction Engineering*, 4th ed. New Jersey: Prentice Hall PTR, 1999.
12. Sanderson RV, Chien HHY. Simultaneous chemical and phase equilibrium calculation. *Ind Eng Chem Process Des Dev*. 1973; 12(1):81–85.
13. Ewa B-W, Jürgen G. Transesterification of methyl acetate and n-butanol catalyzed by Amberlyst 15. *Ind Eng Chem Res*. 2006;45(20): 6648–6654.
14. Kandiyoti R. *Fundamentals of Reaction Engineering*. Rafael Kandiyoti & Ventus Publishing ApS; 2009.
15. Kooijman HA, Taylor R. *The ChemSep Book*, 2nd ed. Norderstedt, Germany: Books on Demand GmbH, 2006.
16. Xiao Y, Gao L, Xiao G, Lv J. Kinetics of the transesterification reaction catalyzed by solid base in a fixed-bed reactor. *Energy Fuels*. 2010;24(11):5829–5833.
17. Hsieh LS, Kumar U, Wu JCS. Continuous production of biodiesel in a packed-bed reactor using shell-core structural Ca(C 3H 7O 3) 2/ CaCO 3 catalyst. *Chem Eng J*. 2010;158(2):250–256.
18. Granath KA, Kvist BE. Molecular weight distribution analysis by gel chromatography on sephadex. *J Chromatogr A*. 1967;28(0): 69–81.
19. Lau HLN, Puah CW, Choo YM, Ma AN, Chuah CH. Simultaneous quantification of free fatty acids, free sterols, squalene, and acylglycerol molecular species in palm oil by high-temperature gas chromatography-flame ionization detection. *Lipids*. 2005;40(5):523–528.
20. Antoniosi Filho NR, Carrilho E, Lancas FM. Fast quantitative analysis of soybean oil in olive oil by high-temperature capillary gas chromatography. *J Am Oil Chem Soc*. 1993;70:1051–1053.
21. Kuksis A, Myher JJ, Geher K. Quantification of plasma lipids by gas-liquid chromatrography on high temperature polarizable capillary columns. *J Lipids Res*. 1993;34:1029–1038.
22. Goto S, Tagawa T, Yusoff A. Kinetics of the esterification of palmitic acid with isobutyl alcohol. *Int J Chem Kinetics*. 1991;23(1): 17–26.
23. Hassan SZ, Vinjamur M. Analysis of sensitivity of equilibrium constant to reaction conditions for esterification of fatty acids with alcohols. *Ind Eng Chem Res*. 2012;52(3):1205–1215.
24. Forsythe T, Parsons R. Chemical equilibrium. In: Robinson S, editor. *CK-12 Chemistry*. Vol. 2, Chapter 19. CK-12 Foundation, 2010.
25. Cooper GM. Metabolic energy. *The Cell. A Molecular Approach*, 2nd ed. United States: Sinauer Associates, 2000.
26. Lower S. Thermodynamic of chemical equilibrium. 2007. Available at: http://www.chem1.com/acad/webtext/thermeq/TE5.html. Accessed on March 12, 2014.

APPENDIX

Table A1. Experimental CPE Data for the Six-Component System in the Bulk Phase, MEOH- and Oil-Rich Phase for Figure a

Bulk Phase (Mass Fraction, $z_{i,\mathrm{exp}}$)						MEOH-Rich Phase (Phase I) (Mass Fraction, $x^{\mathrm{I}}_{i,\mathrm{exp}}$)						Oil-Rich Phase (Phase II) (Mass Fraction, $x^{\mathrm{II}}_{i,\mathrm{exp}}$)					
TG	DG	MG	GLY	MEOH	FAME	TG	DG	MG	GLY	MEOH	FAME	TG	DG	MG	GLY	MEOH	FAME
0.354	0.087	0.001	0.001	0.529	0.027	ND	0.003	0.001	0.003	0.974	0.019	0.728	0.174	0.001	ND	0.061	0.036
0.355	0.095	0.003	0.002	0.527	0.018	ND	0.014	0.004	0.004	0.963	0.014	0.731	0.182	0.001	ND	0.065	0.022
0.353	0.091	0.002	0.001	0.525	0.027	ND	0.009	0.003	0.003	0.955	0.030	0.733	0.180	0.001	ND	0.062	0.023
0.373	0.103	0.004	0.003	0.506	0.011	0.001	0.031	0.007	0.006	0.948	0.007	0.744	0.174	0.001	ND	0.065	0.016
0.345	0.124	0.003	0.002	0.513	0.012	0.001	0.034	0.006	0.005	0.947	0.007	0.697	0.216	0.001	ND	0.069	0.017
0.351	0.113	0.004	0.002	0.522	0.008	0.001	0.035	0.006	0.004	0.948	0.005	0.722	0.196	0.001	ND	0.069	0.011
0.394	0.105	0.002	0.002	0.494	0.002	0.002	0.038	0.005	0.004	0.947	0.004	0.760	0.168	ND	ND	0.072	ND
0.380	0.116	0.003	0.001	0.499	0.002	0.002	0.039	0.005	0.002	0.948	0.004	0.740	0.189	ND	ND	0.071	ND
0.355	0.122	0.004	0.001	0.512	0.006	0.002	0.039	0.007	0.002	0.946	0.004	0.713	0.207	0.001	ND	0.072	0.007

*ND, Nondetectable.

Table A2. Predicted CPE Data for the Six-Component System in the MEOH- and Oil-Rich Phase for Figure a

MEOH-Rich Phase (Phase I) (Mass Fraction, $x^{\mathrm{I}}_{i,\mathrm{calc}}$)						Oil-Rich Phase (Phase II) (Mass Fraction, $x^{\mathrm{II}}_{i,\mathrm{calc}}$)					
TG	DG	MG	GLY	MEOH	FAME	TG	DG	MG	GLY	MEOH	FAME
0.000	0.003	0.000	0.002	0.988	0.007	0.720	0.173	0.002	0.000	0.056	0.048
0.000	0.002	0.000	0.003	0.992	0.003	0.676	0.180	0.005	0.001	0.106	0.031
0.000	0.002	0.000	0.002	0.993	0.004	0.640	0.164	0.003	0.001	0.146	0.046
0.000	0.006	0.000	0.004	0.987	0.003	0.689	0.185	0.007	0.002	0.099	0.019
0.000	0.002	0.000	0.003	0.994	0.001	0.610	0.218	0.006	0.002	0.144	0.020
0.000	0.007	0.000	0.004	0.987	0.003	0.697	0.218	0.007	0.001	0.063	0.014
0.000	0.018	0.000	0.003	0.977	0.001	0.753	0.184	0.004	0.001	0.055	0.003
0.000	0.010	0.000	0.002	0.988	0.001	0.715	0.210	0.005	0.000	0.067	0.003
0.000	0.005	0.000	0.001	0.992	0.001	0.676	0.229	0.007	0.000	0.078	0.009

*Any absolute zero obtained in the simulation data represents non-detectable in the experiment.

Table A3. Experimental CPE Data for the Six-Component System in the Bulk Phase, MEOH-, and Oil-Rich Phase for Figure b

Bulk Phase (Mass Fraction, $z_{i,\mathrm{exp}}$)						MEOH-Rich Phase (Phase I) (Mass Fraction, $x^{\mathrm{I}}_{i,\mathrm{exp}}$)						Oil-Rich Phase (Phase II) (Mass Fraction, $x^{\mathrm{II}}_{i,\mathrm{exp}}$)					
TG	DG	MG	GLY	MEOH	FAME	TG	DG	MG	GLY	MEOH	FAME	TG	DG	MG	GLY	MEOH	FAME
0.387	0.020	0.001	0.002	0.560	0.030	ND	0.002	0.002	0.003	0.961	0.032	0.853	0.041	ND	ND	0.077	0.028
0.430	0.030	0.005	0.006	0.514	0.015	ND	0.007	0.009	0.013	0.962	0.009	0.870	0.053	0.001	ND	0.056	0.021
0.413	0.026	0.001	0.001	0.534	0.025	ND	0.001	0.001	0.002	0.972	0.024	0.841	0.052	0.001	ND	0.080	0.026
0.444	0.026	0.005	0.005	0.508	0.012	ND	0.007	0.009	0.011	0.966	0.007	0.858	0.043	0.001	ND	0.082	0.016
0.392	0.021	0.001	0.001	0.560	0.024	ND	0.001	0.002	0.002	0.968	0.026	0.792	0.042	0.001	ND	0.145	0.021
0.367	0.027	0.006	0.005	0.587	0.008	ND	0.009	0.010	0.011	0.964	0.006	0.741	0.045	0.001	ND	0.203	0.010
0.355	0.031	0.006	0.005	0.597	0.007	ND	0.010	0.011	0.009	0.965	0.006	0.718	0.052	0.001	ND	0.221	0.008

*ND, Nondetectable.

Table A4. Predicted CPE Data for the Six-Component System in the MEOH- and Oil-Rich Phase for Figure b

MEOH-Rich Phase (Phase I) (Mass Fraction, $x^{\mathrm{I}}_{i,\mathrm{calc}}$)						Oil-Rich Phase (Phase II) (Mass Fraction, $x^{\mathrm{II}}_{i,\mathrm{calc}}$)					
TG	DG	MG	GLY	MEOH	FAME	TG	DG	MG	GLY	MEOH	FAME
0.000	0.021	0.000	0.003	0.952	0.024	0.879	0.019	0.003	0.001	0.061	0.038
0.000	0.022	0.000	0.009	0.960	0.008	0.828	0.036	0.009	0.004	0.102	0.021
0.000	0.010	0.000	0.001	0.980	0.009	0.774	0.040	0.002	0.001	0.143	0.039
0.000	0.020	0.000	0.008	0.965	0.007	0.846	0.031	0.009	0.003	0.095	0.016
0.000	0.006	0.000	0.001	0.984	0.008	0.763	0.036	0.002	0.001	0.160	0.038
0.000	0.011	0.000	0.008	0.975	0.005	0.847	0.047	0.012	0.002	0.079	0.012
0.000	0.011	0.000	0.007	0.978	0.004	0.837	0.058	0.013	0.002	0.080	0.010

*Any absolute zero obtained in the simulation data represents non-detectable in the experiment.

Table A5. Experimental CPE Data for the Six-Component System in the Bulk Phase, MEOH- and Oil-Rich Phase for Figure c

Bulk Phase (Mass Fraction, $z_{i,\text{exp}}$)						MEOH-Rich Phase (Phase I) (Mass Fraction, $x^{\text{I}}_{i,\text{exp}}$)						Oil-Rich Phase (Phase II) (Mass Fraction, $x^{\text{II}}_{i,\text{exp}}$)					
TG	DG	MG	GLY	MEOH	FAME	TG	DG	MG	GLY	MEOH	FAME	TG	DG	MG	GLY	MEOH	FAME
0.382	0.028	ND	0.003	0.552	0.034	ND	ND	ND	0.005	0.963	0.032	0.842	0.061	0.001	0.001	0.057	0.038
0.104	0.019	0.003	0.011	0.480	0.383	ND	ND	0.001	0.018	0.807	0.174	0.228	0.041	0.005	0.003	0.093	0.629
0.067	0.016	0.003	0.042	0.459	0.412	ND	ND	0.001	0.077	0.700	0.222	0.149	0.035	0.006	0.001	0.167	0.643
0.017	0.006	0.005	0.010	0.502	0.459	ND	ND	0.004	0.016	0.828	0.151	0.038	0.014	0.008	0.003	0.093	0.845
0.005	0.002	0.004	0.022	0.480	0.486	ND	ND	0.003	0.039	0.728	0.230	0.012	0.005	0.005	0.002	0.177	0.800
0.382	0.028	ND	0.003	0.552	0.034	ND	ND	ND	0.005	0.963	0.032	0.842	0.061	0.001	0.001	0.057	0.038
0.104	0.019	0.003	0.011	0.480	0.383	ND	ND	0.001	0.018	0.807	0.174	0.228	0.041	0.005	0.003	0.093	0.629
0.067	0.016	0.003	0.042	0.459	0.412	ND	ND	0.001	0.077	0.700	0.222	0.149	0.035	0.006	0.001	0.167	0.643

*ND, Nondetectable.

Table A6. Predicted CPE Data for the Six-Component System in the MEOH- and Oil-Rich Phase for Figure c

MEOH-Rich Phase (Phase I) (Mass Fraction, $x^{\text{I}}_{i,\text{calc}}$)						Oil-Rich Phase (Phase II) (Mass Fraction, $x^{\text{II}}_{i,\text{calc}}$)					
TG	DG	MG	GLY	MEOH	FAME	TG	DG	MG	GLY	MEOH	FAME
0.000	0.020	0.000	0.005	0.952	0.023	0.850	0.038	0.001	0.001	0.062	0.048
0.000	0.000	0.000	0.017	0.925	0.058	0.197	0.036	0.005	0.006	0.086	0.670
0.000	0.000	0.001	0.061	0.839	0.099	0.126	0.029	0.005	0.026	0.127	0.686
0.000	0.000	0.001	0.015	0.942	0.041	0.032	0.013	0.009	0.006	0.088	0.852
0.000	0.000	0.001	0.032	0.881	0.086	0.010	0.004	0.006	0.014	0.134	0.831
0.000	0.020	0.000	0.005	0.952	0.023	0.850	0.038	0.001	0.001	0.062	0.048
0.000	0.000	0.000	0.017	0.925	0.058	0.197	0.036	0.005	0.006	0.086	0.670
0.000	0.000	0.001	0.061	0.839	0.099	0.126	0.029	0.005	0.026	0.127	0.686

*Any absolute zero obtained in the simulation data represents nondetectable in the experiment.

Manuscript received July 10, 2014, and revision received Mar. 13, 2015.